UNITED STATES DEPARTMENT OF THE INTERIOR

GEOLOGICAL SURVEY

Thermal conductivity of samples from borehole VC-1, Valles Caldera, New Mexico

by

Robert J. Munroe[1] and J. H. Sass[2]

Open-File Report 87-184

[1]U.S. Geological Survey, Menlo Park, CA 94025
[2]U.S. Geological Survey, Flagstaff, AZ 86001

1987

Abstract

The thermal conductivities of 55 carefully preserved core samples from borehole, VC-1, Valles Caldera, New Mexico, were measured using a combination of methods, the steady-state divided bar and two transient line-source methods. The choice of method was dictated by the physical condition and mechanical strength of the core. Because the well encountered high temperatures (~160°C at the bottom) the room-temperature values of thermal conductivity were corrected using published values for the temperature coefficient of conductivity. A few samples were measured at temperatures of ~100°C as a check on the validity of the published corrections.

INTRODUCTION

In the summer of 1984, the U.S. Department of Energy/Office of Basic Sciences, and the Los Alamos National Laboratory (LANL) coordinated the drilling of a 856 m corehole in the southern ring-fracture zone of the Valles Caldera, New Mexico (Figure 1). The objectives of the corehole were to investigate the hydrothermal system, structure, and stratigraphy of the caldera (see Goff and others, 1986). As part of these investigations, temperatures were measured by LANL in the corehole, and the thermal conductivities of samples of the core were measured by the USGS in the laboratory.

This report summarizes the thermal conductivity measurements together with some preliminary interpretative remarks.

Acknowledgments. The needle probe and half-space probe thermal conductivity measurements were made by Eugene Smith. We thank Paul Morgan for a review of the draft manuscript.

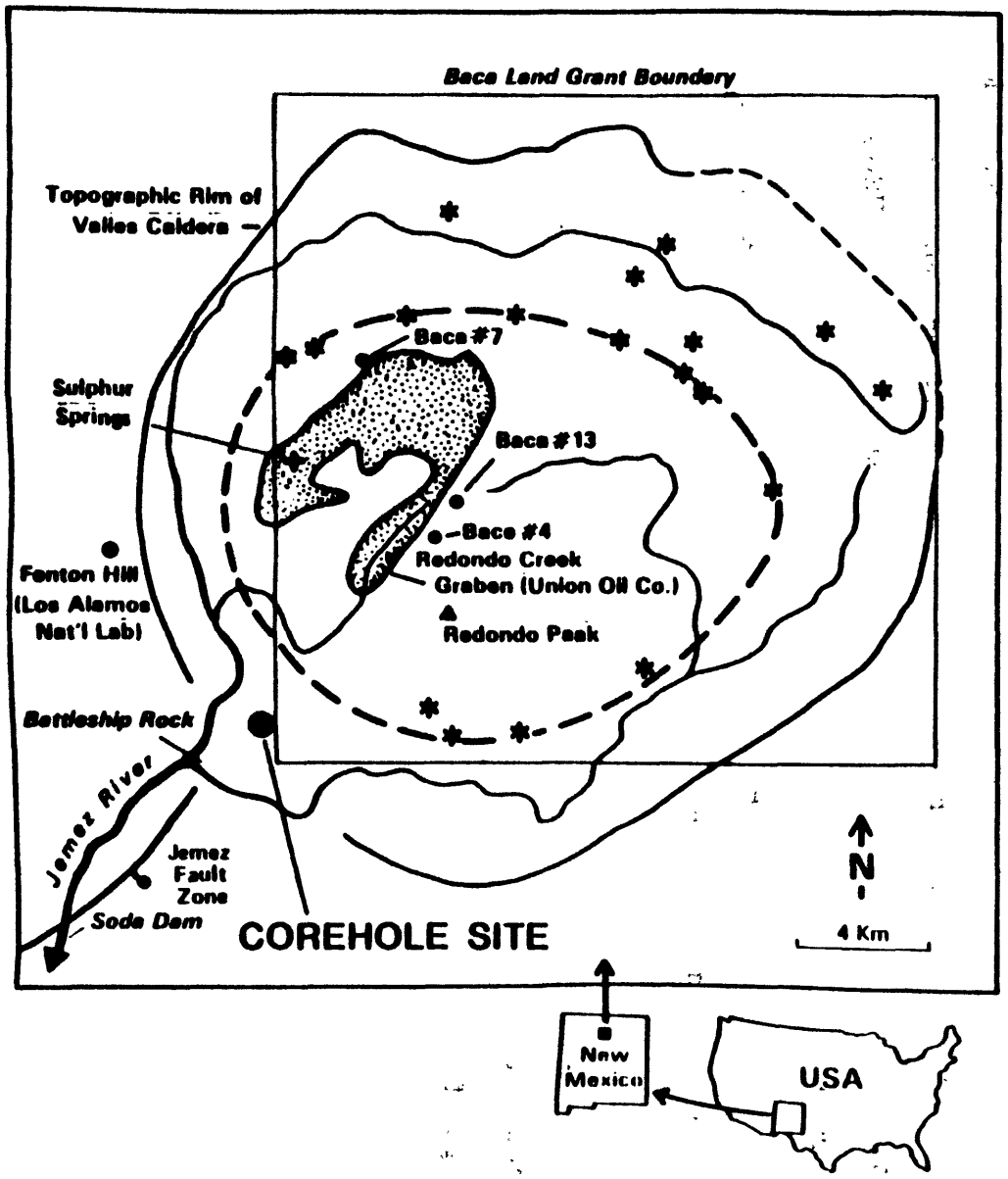

Figure 1. Map showing location of hole VC-1 and some adjacent wells and features (from Goff and others, 1986).

THERMAL CONDUCTIVITY

The corehole, VC-1, penetrated a sequence of volcanic tuff and obsidian layers near the surface, followed by clay and limestone horizons (Goff and others, 1986). The hole bottomed in a sandstone and conglomerate (Figure 2). Core recovery was better than 95%. The samples of the core for thermal conductivity measurements were preserved at the drill site by wrapping them in aluminum foil and then coating them with molten wax.

Thermal conductivity measurements were made with the divided-bar and needle-probe methods (Sass and others, 1971), and with the half-space probe method (Sass and others, 1984). The choice of method was dictated by the physical condition and mechanical strength of the core. Strong, competent rocks were machined into disks for measurement by the divided-bar method. More friable rocks were drilled axially and radially for needle-probe determinations. Rocks that could not be drilled or machined were lapped flat for the line-source half-space apparatus. The results of the measurements are summarized in Table 1.

Disks for the divided-bar method were prepared from the more competent samples of a few of the tuffs, the Madera Limestone and the Sandia sandstone. The measured conductivity of these samples tends to be higher than the less competent samples. For most of the samples, the conductivity was measured using the needle-probe or half-space probe methods.

It is possible to determine the degree of anisotropy in the conductivity of the samples from needle-probe measurements. As the needle-probe method is based on the theory of a line source of heat in an infinite medium, the conductivity of the sample is measured in a direction perpendicular to the long axis of the probe. By comparing the conductivities measured with the probe orientation along the core axis (λ_A) to those with probe along a radius

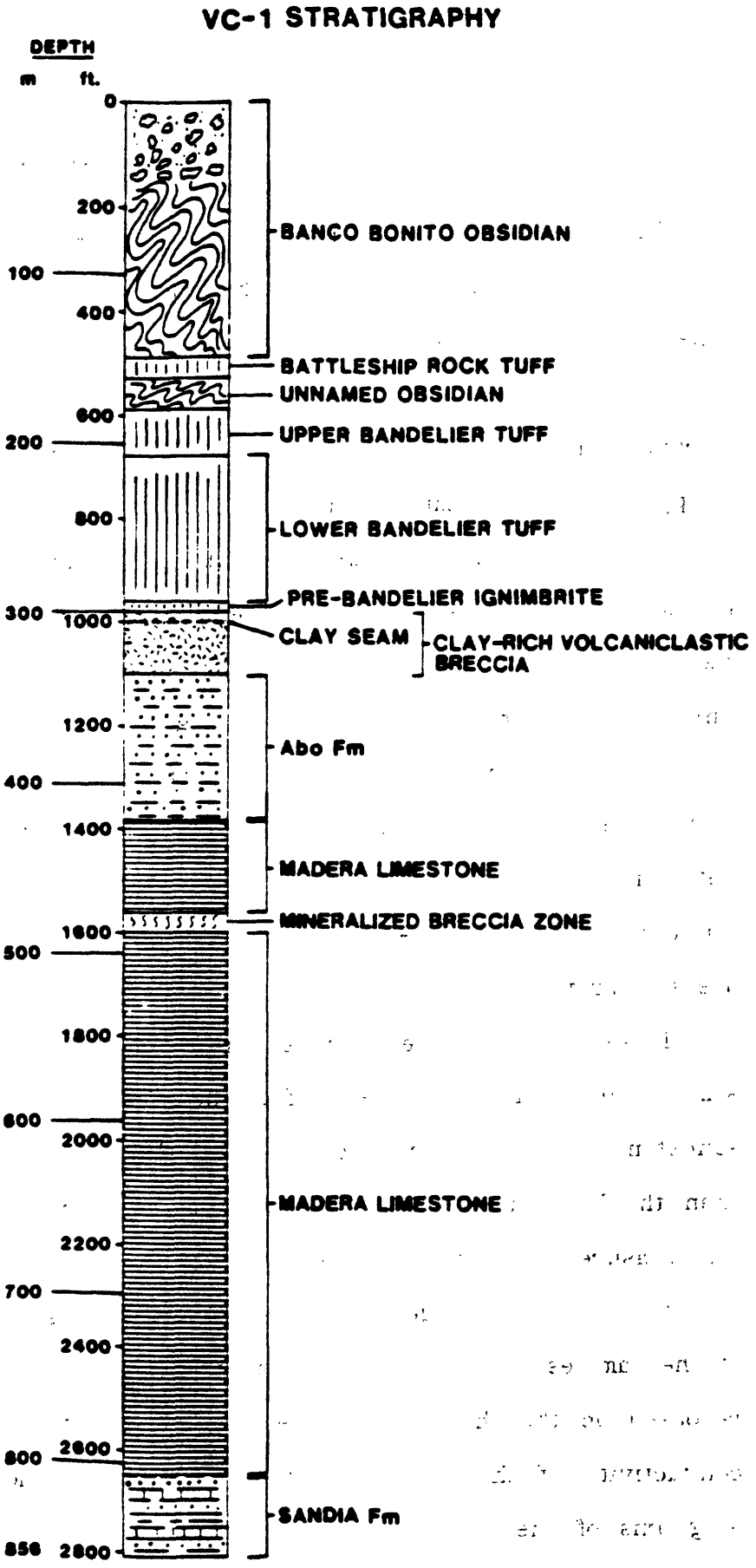

Figure 2. Stratigraphic section from VC-1 (from Goff and others, 1986).

TABLE 1. Thermal conductivity, density and porosity of samples from VC-1

Formation	Depth (m)	Thermal conductivity $\lambda(Wm^{-1}K^{-1})$	Density $\rho(g/cm^3)$	Porosity $\phi(\%)$	Orientation of probe[4]	Temperature[3] °C
Banco Bonito Obsidian	14.4- 14.3	1.03			R	
		0.89			A	
	29.6- 29.7	1.11			R	
		1.07			A	
	47.6-47.8	1.17			R	
		1.14			A	
	60.4- 60.5	1.53			R	
	79.6- 79.8	1.93[1]	2.42	5.2		
	91.8-92.0	1.55			R	
		1.62			A	
	105.6-105.8	1.91[1]	2.35	5.3		
	119.7-119.9	1.29			R	
		1.22			A	
Battleship Rock Tuff	153.7-153.8	0.88			R	
		0.67			A	
Obsidian	170.3-170.5	1.21			R	
		1.16			A	
Upper Bandelier Tuff	182.4-182.6	1.00			R	
		0.93			A	
	201.8-202.0	0.80			R	
		0.87			A	
Lower Bandelier Tuff	214.2-214.3	1.02			A	
	231.1-231.2	1.12			R	
		1.10			A	
	245.5-245.7	1.21			R	
		1.24			A	
	258.0-258.1	1.25			R	
		1.23				
	276.1-276.3	1.15			R	
		1.08			A	

TABLE 1. Thermal conductivity, density and porosity of samples from VC-1 (continued)

Formation	Depth (m)	Thermal conductivity $\lambda(Wm^{-1}K^{-1})$	Density $\rho(g/cm^3)$	Porosity $\phi(\%)$	Orientation of probe[4]	Temperature[3] °C
	289.7-290.0	1.02			R	
		1.04			A	
Volcano-clastic Breccia	304.4-304.6	1.60			R	
		1.65			A	
	318.7-318.9	1.70			R	
		1.98			A	
Abo Formation	334.9-335.1	3.27[1]	2.57	4.6		
	348.5-348.7	1.98			R	
		2.14			A	
	364.8-364.9	1.92			R	
		2.10			A	
	383.7-383.8	1.89			R	
		2.02			A	
	395.6-395.7	1.95			R	
		2.21			A	
	411.5-411.7	1.91			R	
		2.24			A	
	424.9-425.1	2.45			R	
		2.83			A	
	444.0-444.2	1.94			R	
		2.36			A	
	456.4-456.6	2.26			R	
		2.58			A	
	477.7-477.9	2.54			R	
		2.54			A	
Madera Limestone	488.5-488.9	3.41[2]			R	
	502.6-502.9	2.72[2]			R	
	515.7-516.0	2.14			R	
		2.86			A	

TABLE 1. Thermal conductivity, density and porosity of samples from VC-1 (continued)

Formation	Depth (m)	Thermal conductivity $\lambda(Wm^{-1}K^{-1})$	Density $\rho(g/cm^3)$	Porosity $\phi(\%)$	Orientation of probe[4]	Temperature[3] °C
Madera Limestone	532.2-532.5	2.30			R	
		2.58			A	
	551.5-551.7	2.21			R	
		2.30			A	
		2.04			R	42
		2.10			R	52
		2.03			R	60
		2.01			R	76
		2.03			R	90
		2.09			R	102
		1.88			R	106
	568.7-568.9	2.56			R	
		2.18			A	
		2.12			R	92
		2.14			R	103
	581.5-581.8	2.55			R	
		3.18			A	
	593.8-594.2	2.94			R	
		2.98			A	
	607.8-608.1	2.74			R	
		2.53			A	
	626.8-627.0	3.04			R	
		3.03			A	
	639.4-639.5	2.71			R	
		3.21			A	
		3.16			A	45
		2.96			A	60
		3.06			A	76
		2.87			A	91
		2.91			A	110
	652.8-653.1	3.00			R	
		3.19			A	
	672.4-672.6	2.91			R	
		3.07			A	

TABLE 1. Thermal conductivity, density and porosity of samples from VC-1 (continued)

Formation	Depth (m)	Thermal conductivity $\lambda(Wm^{-1}K^{-1})$	Density $\rho(g/cm^3)$	Porosity $\phi(\%)$	Orientation of probe[4]	Temperature[3] °C
Madera Limestone	684.5-684.7	2.44			R	
		3.24			A	
		1.93			A	50
		2.65			A	55
		2.69			A	66
		2.68			A	87
		2.57			A	99
	704.0-704.2	3.27[1]	2.56	6.7		
	715.4-715.6	2.91			R	
		2.85			A	
	732.8-733.0	3.57[1]	2.64	1.2		
	749.4-749.7	3.07[1]	2.65	2.2		
	761.8-762.1	3.05			R	
		3.31			A	
	777.8-778.0	4.31[1]	2.55	8.6		
	790.3-790.5	2.72			R	
	809.5-809.6	4.06[1]	2.50	7.9		
Sandia	819.9-820.2	2.72			R	
		2.90			A	
	838.4-838.5	2.44			R	
Formation		2.72			A	
	852.0-852.2	1.75			R	

All thermal conductivity measurements made using the needle-probe method except:

[1]Measurements using the divided bar.
[2]Measurements using the half-space probe.
[3]All thermal conductivity measurements made between 19°C and 28°C except where noted.
[4]Needle-probe orientation: R long axis radial to core
A long axis parallel to core

(λ_R) any anisotropy in conductivity is apparent. Above the Abo formation, most of the rocks sampled by the needle probe are isotropic with regards to the conductivity since $\lambda_A \cong \lambda_R$ for each sample. Since these beds are essentially horizontal, the vertical conductivity is the conductivity perpendicular to the bedding, λ_S, and is

$$\lambda_S = \lambda_R = \lambda_A \quad .$$

The low conductivities measured for these rocks probably result from incomplete saturation as they are above the water table. The rocks of the Abo Formation, Madera Limestone and Sandia Formation, however, dip 25° S.E. For disks used with the divided-bar method, the measured conductivity is the vertical component of the conductivity. For the less competent core, the effect of the dip on the conductivity may be determined from measurements made with a needle probe oriented vertically and horizontally in the core. If λ_A and λ_R are the measured vertical and horizontal conductivities, λ_1 and λ_3 the conductivities parallel and perpendicular to the bedding and λ_S the vertical component of conductivity, then from Grubbe et al. (1983)

$$\lambda_1 = \lambda_R^2 + \frac{\lambda_A^2 - \lambda_R^2}{\cos^2\gamma}$$

$$\lambda_3 = \frac{\lambda_R^2}{\lambda_1}$$

$$\lambda_S = \lambda_1 + (\lambda_3 - \lambda_1) \sin^2\gamma$$

where γ is the dip angle. It is assumed that the conductivity is isotropic in the plane of the bedding. The anisotropy in the conductivity is λ_1/λ_3. The vertical component of conductivity, λ_S, and anisotropy λ_1/λ_3 are listed in Table 2 for the needle-probe measurements for which both λ_A and λ_R were

TABLE 2. Vertical component of thermal conductivity (λ_S) of samples from Paleozoic section of VC-1 derived from measured values

Formation	Depth (m)	Thermal conductivity, $Wm^{-1}K^{-1}$				Anisotropy	
		λ_R	λ_A	λ_1	λ_3	λ_1/λ_3	λ_S
Abo	348.5-348.7	1.98	2.14	2.17	1.81	1.20	2.11
	364.8-364.9	1.92	2.10	2.14	1.72	1.24	2.06
	383.7-383.8	1.89	2.02	2.05	1.74	1.18	1.99
	395.6-395.7	1.95	2.21	2.26	1.68	1.34	2.16
	411.5-411.7	1.91	2.24	2.31	1.58	1.46	2.18
Madera Limestone	424.9-425.1	2.45	2.83	2.91	2.07	1.41	2.76
	444.0-444.2	1.94	2.36	2.44	1.54	1.58	2.28
	456.4-456.6	2.26	2.58	2.65	1.93	1.37	2.52
	477.7-477.9	2.54	2.54			1.00	2.54
	515.7-516.0	2.14	2.86	2.99	1.53	1.96	2.73
	532.2-532.5	2.30	2.58	2.64	2.01	1.32	2.53
	551.5-551.7	2.21	2.30	2.32	2.11	1.10	2.28
	568.7-568.9	2.56	2.18	2.09	3.14	0.67	2.28
	581.5-581.8	2.55	3.18	3.30	1.97	1.67	3.06
	593.8-594.2	2.94	2.98	2.99	2.89	1.03	2.97
	607.8-608.1	2.74	2.53	2.48	3.03	0.82	2.58
	626.8-627.0	3.04	3.03			1.00	3.04
	639.4-639.5	2.71	3.21	3.31	2.22	1.49	3.11
	652.8-653.1	3.00	3.19	3.23	2.79	1.16	3.15
	672.4-672.6	2.91	3.07	3.10	2.73	1.14	3.03
	684.5-684.7	2.44	3.24	3.39	1.76	1.93	3.10
	715.4-715.6	2.91	2.85	2.84	2.99	0.95	2.87
	761.8-762.1	3.05	3.31	3.36	2.76	1.22	3.25
Sandia	819.9-820.2	2.72	2.90	2.94	2.52	1.17	2.86
	838.4-838.5	2.44	2.72	2.78	2.14	1.30	2.66

TABLE 3. Harmonic mean formation thermal conductivities for samples from VC-1

Formation	Depth, m	Mean formation temp., °C	N	Harmonic mean thermal conductivity, $Wm^{-1}K^{-1}$		Anisotropy
				at 25°C	Corrected to mean formation temperature	
Intracaldera volcanic sequence	0 to 298	35	32	1.11±0.04	1.11±0.04	
Sheared clay-rich volcanic colluvium and/or debris flow	298 to 333	70	4	1.72±0.08	1.72±0.08	
Abo	333 to 422	83	6	2.23±0.14	2.08±0.13	1.24
Madera Limestone	422 to 808	140	22	2.86±0.09	2.50±0.08	1.28
Sandia	808 to 856	165	3	3.10±0.38	2.64±0.33	1.24

made. The harmonic means of the vertical components of the conductivities from both the divided bar and needle-probe measurements, for each formation, measured at 25°C, are given in Table 3.

To determine the variation of the conductivity of the rocks with temperature, the conductivities of four samples of the Madera Limestone were measured at increasing temperatures. The results of these measurements are given in Table 1. The harmonic means of the room temperature conductivities, adjusted to average formation temperatures using temperature coefficients of thermal resistivity determined by Birch and Clark (1940) for rocks of similar mineralogy, appear in Table 3. The harmonic mean conductivity for all samples of the Madera Limestone adjusted to 100°C (2.60 $Wm^{-1}K^{-1}$) is somewhat higher than the mean of four needle-probe measurements at 98°C (2.39 $Wm^{-1}K^{-1}$). This systematic difference probably results from the fact that the less competent material measured by the needle-probe method has a lower conductivity than those samples measured with the divided-bar, which are not represented by the high-temperature measurements (Table 1).

SUMMARY

Thermal conductivity of rocks from corehole VC-1 were measured by a combination of the divided-bar, needle-probe and half-space probe methods. Sufficient measurements were obtained to characterize the thermal conductivity of the major formations encountered and to allow estimation of conductive heat flow from this and other wells penetrating these rocks.

References

Birch, Francis, and Clark, Harry, 1940, The thermal conductivity of rocks and its dependence on temperature and composition: American Journal of Science, v. 238, p. 529-558 and 613-635.

Goff, F., Rowley, J., Gardner, J. N., Hawkins, W., Goff, S., Charles, R., Wachs, D., Maassen, L., and Heiken, G., 1986, Initial results from VC-1, first Continental Scientific Drilling Program Core Hole in Valles Caldera, New Mexico: Journal of Geophysical Research, v. 91, p. 1742-1752.

Grubbe, K., Haenel, R., and Zoth, G., 1983, Determination of the vertical component of thermal conductivity by line-source methods: Zbl. Geol. Palaont. Teil I, p. 49-56.

Sass, J. H., Kennelly, J. P., Jr., Smith, E. P., and Wendt, W. E., 1984, Laboratory line-source methods for the measurement of thermal conductivity of rocks near room temperature: U.S. Geological Survey Open-File Report 84-91, 21 p.

Sass, J. H., Lachenbruch, A. H., Munroe, R. J., Greene, G. W., and Moses, T. H., Jr., 1971, Heat flow in the western United States: Journal of Geophysical Research, v. 76, p. 6376-6413.